HAL
open science

Ln3[SiON3]O (Ln = La, Ce, Pr) – Three Oxonitridosilicate Oxides with Crystal Structures Derived from the Anti-Perovskite Structure Type

Juliane Kechele, Christian Schmolke, Saskia Lupart, Wolfgang Schnick

To cite this version:

Juliane Kechele, Christian Schmolke, Saskia Lupart, Wolfgang Schnick. Ln3[SiON3]O (Ln = La, Ce, Pr) – Three Oxonitridosilicate Oxides with Crystal Structures Derived from the Anti-Perovskite Structure Type. Journal of Inorganic and General Chemistry / Zeitschrift für anorganische und allgemeine Chemie, 2009, 636 (1), pp.176. 10.1002/zaac.200900274 . hal-00507773

HAL Id: hal-00507773

https://hal.science/hal-00507773v1

Submitted on 31 Jul 2010

HAL is a multi-disciplinary open access archive for the deposit and dissemination of scientific research documents, whether they are published or not. The documents may come from teaching and research institutions in France or abroad, or from public or private research centers.

L'archive ouverte pluridisciplinaire **HAL**, est destinée au dépôt et à la diffusion de documents scientifiques de niveau recherche, publiés ou non, émanant des établissements d'enseignement et de recherche français ou étrangers, des laboratoires publics ou privés.

Zeitschrift für Anorganische und Allgemeine Chemie

Ln3[SiON3]O (Ln = La, Ce, Pr) – Three Oxonitridosilicate Oxides with Crystal Structures Derived from the Anti-Perovskite Structure Type

Journal:	*Zeitschrift für Anorganische und Allgemeine Chemie*
Manuscript ID:	zaac.200900274.R1
Wiley - Manuscript type:	Article
Date Submitted by the Author:	25-May-2009
Complete List of Authors:	Kechele, Juliane; Ludwig-Maximilians-Universitaet Muenchen, Department Chemie und Biochemie Schmolke, Christian; Ludwig-Maximilians-Universitaet Muenchen, Department Chemie und Biochemie Lupart, Saskia; Ludwig-Maximilians-Universitaet Muenchen, Department Chemie und Biochemie Schnick, Wolfgang; Ludwig-Maximilians-Universitaet Muenchen, Department Chemie und Biochemie
Keywords:	Magnetic properties, Oxonitridosilicate oxide, Solid-state NMR, Rietveld refinement, Structure elucidation

scholarONE™ Manuscript Central

$Ln_3[SiON_3]O$ (Ln = La, Ce, Pr) – Three Oxonitridosilicate Oxides with Crystal Structures Derived from the Anti-Perovskite Structure Type

Juliane A. Kechele, Christian Schmolke, Saskia Lupart, and Wolfgang Schnick *

Department Chemie und Biochemie der Ludwig-Maximilians-Universität München

Received …

* Prof. Dr. W. Schnick
Department Chemie und Biochemie
Lehrstuhl für Anorganische Festkörperchemie
Ludwig–Maximilians–Universität München
Butenandtstraße 5 – 13 (D)
D–81377 München, Germany
Fax: +49–(0)89–2180–77440
E–mail: wolfgang.schnick@uni–muenchen.de

Abstract

The oxonitridosilicate oxides $Ln_3[SiON_3]O$ with Ln = La, Ce, Pr were obtained by high-temperature syntheses (1450 - 1600 °C) in a radio-frequency furnace. The crystal structures were determined from single-crystal X-ray diffraction data and confirmed by Rietveld refinements. The compounds $Ln_3[SiON_3]O$ crystallize in space group *I*4/*mcm* ($La_3[SiON_3]O$: $a = 6.8224(10)$, $c = 11.074(2)$ Å, $Z = 4$; $R1 = 0.0240$; $Ce_3[SiON_3]O$: $a = 6.7233(10)$, $c = 11.069(2)$ Å, $Z = 4$, $R1 = 0.0234$; $Pr_3[SiON_3]O$: $a = 6.6979(9)$, $c = 11.005(2)$ Å, $Z = 4$; $R1 = 0.0156$) and they were found to be isotypic with $Gd_3[SiON_3]O$, whose structure derives from the anti-perovskite structure type. In the crystal there are elongated OLn_6-octahedra which are interconnected through common vertices. In the cavities of this network there are exclusively non-condensed $SiON_3$ tetrahedra. ^{29}Si solid-state NMR investigations, lattice energy calculations (MAPLE) and EDX measurements confirmed the crystal structure and the chemical compositions. For $Ce_3[SiON_3]O$, magnetic susceptibility measurements were carried out and the paramagnetic behavior with an experimental magnetic moment of 2.2 μ_B per cerium atom indicates Ce^{3+}.

Keywords

Magnetic properties; Oxonitridosilicate oxide; Rietveld refinement; Solid-state NMR; Structure elucidation

Introduction

In the literature there are multitudinous reports on varied possibilities for substitution and distortion in perovskite type materials.[1] In this context, the oxonitridosilicate oxide $Gd_3[SiON_3]O$ [2] has been investigated which is isotypic to $Ba_3[SiO_4]O$ [3,4] and $Cs_3[CoCl_4]Cl$.[5] All three compounds can be derived from the anti-perovskite structure type in a hierarchical sense with tetrahedral building blocks ($SiON_3$, SiO_4, $CoCl_4$) substituting the large alkaline earth ions in perovskite.

Oxonitridosilicates are intermediates between classical oxosilicates and nitridosilicates and can be formally derived by partial substitution of O for N. While oxygen in classical oxosilicates usually occur in a terminal $O^{[1]}$ or simply bridging $O^{[2]}$ function, nitrogen atoms can additionally act as a triply ($N^{[3]}$) or even quadruply ($N^{[4]}$) bridging atom, leading to a manifold of additional structural possibilities. Consequently, nitridosilicates exhibit a more

variable degree of condensation in the range $1 : 4 \leq \kappa \leq 3 : 4$ (i.e. the molar ration Si : (N,O)) as compared to classical oxosilicates ($1 : 4 \leq \kappa \leq 1 : 2$). Due to the enhanced connectivity of $N^{[3]}$ and even $N^{[4]}$ nitrogen atoms, new topological building blocks are possible. For example, in $BaYbSi_4N_7$ a "star-shaped" unit $[N^{[4]}(SiN_3)_4)]$ has been observed for the first time.[6] Here, the quadruply bridging nitrogen atom ($N^{[4]}$) adopts ammonium character. A further structural motif, which is unknown for oxosilicates so far, is the highly-condensed *dreier* ring layer.[7] This kind of layer can be found in the layer oxosilicates $MSi_2O_2N_2$ (M = Ca, Sr, Ba, Eu) [8-11] or it is part of the silicate framework (e.g. in $M_2Si_5N_8$ [12,13] (M = Ca, Sr, Ba), MSi_7N_{10} (M = Sr, Ba)).[14,15] Most structures of (oxo)nitridosilicates analyzed so far, contained a highly condensed framework.[16,17] However, the anionic part of the structure of $Gd_3[SiON_3]O$ contains exclusively non-condensed $SiON_3$ tetrahedra. Further examples for oxonitridosilicates with non-condensed silicate substructure are $Li_6[SiN_2O_2]$,[18] $Ln_{10}[SiO_{3.67}N_{0.33}]_6O_2$ (Ln = La, Nd, Sm, Gd),[19] $M_{10}[SiO_2N_2]_6O_2$ (M = Ti, Ge),[19] and $LnEu[SiO_3N]$ (Ln = La, Nd, Sm).[20]

In this contribution, we report on the syntheses, crystal structures and magnetic properties of $Ln_3[SiON_3]O$ with Ln = La, Ce, Pr. These compounds are isotypic to $Gd_3[SiON_3]O$, which has been described in the literature before.

Results and discussion

Syntheses and sample characterization

As exemplified by the synthesis of $Pr_3[SiON_3]O$, the compounds $Ln_3[SiON_3]O$ (Ln = La, Ce, Pr) can be obtained by various synthetical routes (cf. equation (1) – (5)) at temperatures ranging between 1450 and 1600 °C with varying purity degrees. The metals Ln (La, Ce, Pr), different Ln oxides, silicon diimide, and SiO_2 were used as starting materials for the syntheses. The oxidation state of the Ln in the starting material is apparently irrelevant. Starting from the respective metals leads to intermediate formation of the nitrides LnN (Ln = La, Ce, Pr).

$$10\ La + 4\ La_2O_3 + 6\ \text{“}Si(NH)_2\text{”} + 5\ N_2 \rightarrow 6\ La_3[SiON_3]O + 4\ NH_3 \quad (1)$$

$$12\ Ce + 6\ CeO_2 + 6\ \text{”}Si(NH)_2\text{”} + 5\ N_2 \rightarrow 6\ Ce_3[SiON_3]O + 4\ NH_3 \quad (2)$$

$$126\ Pr + 12\ Pr_6O_{11} + 66\ \text{“}Si(NH)_2\text{”} + 55N_2 \rightarrow 66\ Pr_3[SiON_3]O + 44\ NH_3 \quad (3)$$

$$6\ Pr + 2\ SiO_2 + 3\ N_2 \rightarrow 2\ Pr_3[SiON_3]O \quad (4)$$

$$18\ Pr + 6\ \text{“}Si(NH)_2\text{”} + 3\ O_2 \rightarrow 6\ Pr_3[SiON_3]O + 4\ NH_3 \quad (5)$$

The chemical composition and the phase purity of the samples were confirmed by EDX measurements and Rietveld refinements of the X-ray powder diffraction data (cf. Figure 1).

Crystal structure description

The structure of $Ln_3[SiON_3]O$ (Ln = La, Ce, Pr) is isotypic to $Gd_3[SiON_3]O$, which is derived from the anti-perovskite structure type.[2] In Figure 2, the crystallographic relationship between the two structures is clarified using a group-subgroup scheme. Due to the hierarchical structural relation ($SiON_3$ units substitute for alkaline earth in the perovskite structure type) the complex $SiON_3$ tetrahedra have been approximated by the coordinates of their tetrahedral center (Si).

The crystal structure of the compounds consists of a framework which is built up of exclusively vertex-sharing OLn_6 octahedra (Ln = La, Ce, Pr). These octahedra are elongated along [001] and tilted as compared to the ideal cubic perovskite structure type (cf. Figure 3). The twisting is caused by electrostatic reasons or size effects, as the Ca atoms in the perovskite structure type are substituted by $SiON_3$ tetrahedra in $Ln_3[SiON_3]O$ (Ln = La, Ce, Pr). These $SiON_3$ tetrahedra are exclusively non-condensed and fill the voids of the OLn_6 octahedra framework. A differentiation of the O and N atoms was not possible by X-ray methods, as there is only one crystallographic position for these atoms belonging to the tetrahedra. Thus, the O and N atoms were distributed to the light atom positions on the basis of the crystal structure of the isotypic compound $Gd_3[SiON_3]O$. This distribution was corroborated by lattice energy calculations (MAPLE, Madelung part of lattice energy).[21,22] The results of the calculations based on the O/N distribution in $Gd_3[SiON_3]O$ are summarized in Table 1.

The distances Si-(O,N) (cf. Table 2) are in the typical range for terminal bonds Si-(O,N) in oxonitridosilicates (cf. $La_{16}[Si_8N_{22}][SiON_3]_2$: 1.689(5) - 1.743(8) Å;[25] $Ln_{10}[Si_{10}O_9N_{17}]X$: 1.664(4) - 1.709(7) Å (Ln = Ce, X = Br), 1.666(3) - 1.713(5) Å (Ln = Nd, X = Br), 1.665(3) – 1.718 (5) Å (Ln = Nd, X = Cl);[26] $Pr_{10}[Si_{10-x}Al_xO_{9+x}N_{17-x}]Cl$ ($x \approx 1$): 1.674(7) – 1.739(6) Å).[27] The angles N/O(1)[1]-Si(1)-N/O(1)[1] (cf. Table 2) are close to the regular tetrahedral angle.

The structures of $Ln_3[SiON_3]O$ (Ln = La, Ce, Pr) contain two crystallographically independent Ln^{3+} sites, which are surrounded by eight and ten (N,O) atoms, respectively (cf. Figure 4). The distances Ln-(N,O) (Ln = La, Ce, Pr) are listed in Table 2. Some distances Ln(2)[8]-(N,O) are slightly shorter than the smallest sum of the ionic radii ($La^{[8]}$-O: 2.56 Å; $La^{[8]}$-N: 2.62 Å; $Ce^{[8]}$-O: 2.54 Å; $Ce^{[8]}$-N: 2.60 Å; $Pr^{[8]}$-O: 2.53 Å; $Pr^{[8]}$-N: 2.59 Å)[28] but the distances are in the same range than in other well characterized oxonitrido(alumo)silicates (e.g.: $La_4Si_2O_7N_2$: La-(O,N) 2.298(6) – 2.903(5) Å;[29] $Ce_{10}[Si_{10}O_9N_{17}]Br$: Ce-(O,N) 2.409(4)

– 2.7465(7) Å, Ce-N 2.447(7) – 3.016(5) Å;[26] $Pr_{10}[Si_{10-x}Al_xO_{9+x}N_{17-x}]Cl$ ($x \approx 1$): Pr-(O,N) 2.390(4) – 2.7465(7) Å, Pr-N 2.439(7) – 3.08(5) Å).[27]

The anisotropic displacement parameters of the Ln(1) site are larger by the factor of about 2-3 in comparison with the values of the Ln(2) site (Ln = La, Ce, Pr). Most probably, local deviations from the special site of Ln(1) causes the increase of the parameters. This effect was also observed for $Gd_3[SiON_3]O$.[2]

Furthermore, the displacement ellipsoid of O(2) is elongated, which is presumably due to the deformation of the OLn_6 octahedra (Ln = La, Ce, Pr), mentioned above. Therefore, a splitting of this site was assumed at lower temperatures analogously with the Gd containing compound. A crystal structure investigation for $Ce_3[SiON_3]O$ at 130 K confirmed this assumption.

^{29}Si solid-state NMR

The ^{29}Si solid-state NMR spectrum of $La_3[SiON_3]O$ shows one broad signal peaking at -56.2 ppm with a full width at half maximum of 8 ppm (cf. Figure 5) This broadness of the signal is caused by the quadrupole momentum of the La atoms. The signal corresponds to $SiON_3$ tetrahedra as evidenced by comparable shifts in La containing oxonitridoalumosilicate glasses (-54.4 and -56.0 ppm). For these compounds also the shifts for SiN_4 (-43.3 and -46.9 ppm) and SiN_2O_2 (-64.0, -62.5 and -60.9 ppm) were reported, which are not in the same range.[30] Therefore, the NMR results corroborate that $La_3[SiON_3]O$ exhibits exclusively $SiON_3$ tetrahedra as evidenced by lattice energy calculations (MAPLE).

Magnetical behavior

In the insert of Figure 6 the isothermal magnetization (at 2 and 300 K) of $Ce_3[SiON_3]O$ is depicted. Below the Curie-temperature $T_C \approx 7$ K, a ferromagnetic ordering was observed. The saturation magnetization converges to a value of 3 μ_B per formula unit, which is in accordance with three Ce^{3+} ions per formula unit.

The temperature dependence of the reciprocal magnetic susceptibility is shown in Figure 6. The bending of the reciprocal susceptibility curve is most probably caused by an amorphous by-product, which could not be determined by powder diffraction. Due to crystal field effects a certain deviation from Curie-Weiss behavior is observed. Therefore, the data between 200 and 300 K were fitted with an extended Curie-Weiss equation $\chi_m = \chi_0 + C/(T - \theta)$, which results in an effective magnetic moment of 2.2 μ_B per Ce. The temperature independent part of the susceptibility χ_0 is comparatively large as the crystal field effects are neglected and has

no physical meaning. The magnetic moment is slightly below the theoretical value for free Ce^{3+} (2.54 μ_B). However, most of the experimentally determined values for Ce^{3+} containing compounds have been reported between 2.3 and 2.5 μ_B.[31] Therefore, the measurements corroborate occurrence of solely Ce^{3+} in $Ce_3[SiON_3]O$.

Comparison of $Ln_3[SiON_3]O$ with other A_3BX_5 phases

The *a*/*c* ratio of the compounds $Ln_3[SiON_3]O$ (Ln = La, Ce, Pr, Gd) decreases between La and Gd according to the ionic radii. For the Ce and Pr containing compounds the values are identical within the margin of error, as the two ions have almost identical radii. However, this trend could not be observed for the lattice parameters of the compounds. Therefore, the correlation between the ratio *a*/*c* and the ionic radii is probably caused by an anisotropic framework folding mechanism, which modulates the cavities. The same trend was observed for the deviation of the OLn_6 units from regular octahedral symmetry (Ln = La, Ce, Pr, Gd) (cf. Table 3). A correlation between the *a*/*c* ratio and the distortion of the octahedra could also be observed for isotypic compounds $Cs_3[CoCl_4]Cl$ [5] and $Ba_3[SiO_4]O$.[3,4] However, the tilting angle ξ is independent from the *a*/*c* ratio of the compounds. For $Ln_3[SiON_3]O$ (Ln = La, Ce, Pr, Gd) the values are in the same range, but there is no trend observable according to the ionic radii.

Conclusions

In the last years, (oxo)nitridosilicates have received remarkable attention in materials science, as these compounds are both thermally and chemically very stable. With the syntheses of $Ln_3[SiON_3]O$ (Ln = La, Ce, Pr), oxonitridosilicates with non-condensed tetrahedra could be obtained, although this group of compounds has a stronger tendency to form condensed networks than classical oxosilicates. Due to the non-condensed silicate substructure, the compounds are air- and water sensitive.

Although it was possible to investigate the distribution O/N for the La containing compound by means of solid-state NMR measurements, it would be interesting to precisely determine the distribution using neutron diffraction. However, the available single crystals are yet too small for single-crystal neutron diffraction. Moreover powder data are most probably not conclusive enough, as one crystallographic light atom position has to be occupied statistically with both nitrogen and oxygen atoms and there was no indication for a decrease in symmetry.

Experimental part

Syntheses

Synthesis of silicon diimide "Si(NH)$_2$"

Instead of the relatively unreactive Si_3N_4 silicon diimide was used as starting material. Previous syntheses of several (oxo)nitridosilicates and oxonitridoalumosilicates showed, that "$Si(NH)_2$" is well suited as starting material.[16,17,32] According to equation 1 and 2, the X-ray amorphous and relatively undefined compound was obtained by ammonolysis of $SiCl_4$ (> 98%, Merck, Darmstadt), followed by a thermal treatment at 600 °C under an atmosphere of pure NH_3.

$$SiCl_4 + 6\,NH_3 \xrightarrow[NH_3\ \text{atmosphere}]{-78\ °C} \text{“}Si(NH)_2\text{“} + 4\,NH_4Cl \qquad (6)$$

$$\xrightarrow[NH_3\ \text{atmosphere}]{600\ °C;\ -NH_4Cl} \text{“}Si(NH)_2\text{”} \qquad (7)$$

Synthesis of $La_3[SiON_3]O$

For the synthesis of $La_3[SiON_3]O$ La (231.5 mg, 1.67 mmol, 99.9 %, Smart Elements) as small pieces, silicon diimide (53.8 mg, 0.25 mmol) and La_2O_3 (217.2 mg, 0.67 mmol, 99.999 %, Chempur) were mixed in an agate motar and filled in a tungsten crucible under argon atmosphere in a glove box (Unilab, MBraun, $O_2 \leq 1$ ppm, $H_2O \leq 1$ ppm). Under purified N_2, the crucible was heated to 1600 °C within 1 h in the reactor of a radio-frequency furnace [32] and this maximum temperature was kept for 10 h. Subsequently, the crucible was cooled down to 900 °C with a rate of about 16 °C h^{-1} before quenching to room temperature by switching off the furnace. The sample contains exclusively $La_3[SiON_3]O$ as green-yellow crystals.

Synthesis of $Ce_3[SiON_3]O$

$Ce_3[SiON_3]O$ was synthesized starting from Ce (280.2 mg, 2.0 mmol, 99.9%, Smart Elements) as small pieces, CeO_2 (172.1 mg, 1.0 mmol, 99.99 %, Chempur) and silicon diimide (53.8 mg, 0.25 mmol). After thoroughly mixing the starting materials in an agate mortar, the mixture was filled in a tungsten crucible under argon atmosphere in a glove box (Unilab, MBraun, $O_2 \leq 1$ ppm, $H_2O \leq 1$ ppm). The crucible was heated in a radio-frequency furnace analogously with the synthesis of the La containing compound. $Ce_3[SiON_3]O$ was obtained without any by-products as dark-red crystals.

Synthesis of $Pr_3[SiON_3]O$

$Pr_3[SiON_3]O$ was obtained with varying degrees of purity by diverse synthetical routes using different starting materials. For example, $Pr_4Si_2O_7N_2$ [33] or PrN [34] were observed as by-products. For all syntheses, the starting materials were thoroughly mixed in an agate mortar in a glove box (Unilab, MBraun, $O_2 \leq 1$ ppm, $H_2O \leq 1$ ppm) and subsequently heated in a tungsten crucible in a radio-frequency furnace under purified N_2.

One possibility to synthesize the compound starts from metallic Pr (178.8 mg, 1.27 mmol, 99.9%, Chempur, Karlsruhe) as small pieces, silicon diimide (37.0 mg, 0.17 mmol) and Pr_6O_{11} (110.1 mg, 1.1 mmol, > 99.9 %, Auer Remy, Hamburg). The mixture was heated to 950 °C within 5 min and kept for 25 min. Afterwards the temperature was increased to 1450 °C with a rate of about 42 °C h^{-1} and kept at that temperature for 8 h. Subsequently, the crucible was cooled down to 750 °C with a rate of about 140 °C h^{-1} before switching off the furnace.

For an alternative synthetical route Pr (211.3 mg, 1.5 mmol, 99.9%, Chempur, Karlsruhe) as small pieces and SiO_2 (30.4 mg, 0.5 mmol, ≥ 99.8%, Degussa, Frankfurt/Main) were used as starting materials. The heating program is similar to the program for the synthesis of $La_3[SiON_3]O$, but as maximum temperature 1550 °C was chosen.

$Pr_3[SiON_3]O$ was also observed as product of the reaction between Pr (169.1 mg, 1.2 mmol, 99.9%, Chempur, Karlsruhe) and silicon diimide (53.8 mg; 0.25 mmol). Probably, the starting materials were contamined with oxygen in the latter case. The crucible was heated with the same temperature program as used for the syntheses of $Ln_3[SiON_3]O$ (Ln = La, Ce).

Chemical Analyses

Elemental analyses on selected crystals were performed for all compounds by energy dispersive X-ray spectroscopy (EDX) using a JSM-6500F scanning electron microscope (Jeol) with a Si/Li EDX detector (Oxford Instruments, model 7418). The measurements indicate a molar ratio Ln/Si = 3 : 1 (Ln = La, Ce, Pr), which corroborates the formation of $Ln_3[SiON_3]O$ (Ln = La, Ce, Pr). The determined compositions are in accordance with the structure model within the typical error ranges, as the result for $Pr_3[SiON_3]O$ demonstrates (calc. (at%): Pr 33, Si 11, N 33, O 22; found (at%): Pr 30, Si 9, N 36 O 24).

Single-crystal X-ray analysis

Single crystals of $Ln_3[SiON_3]O$ (Ln = La, Ce, Pr) were isolated, enclosed in glass capillaries (0.2 mm), and sealed under argon atmosphere. Initially, the crystals were examined by Laue photographs recorded on a Bueger camera equipped with an image plate system. Single-crystal X-ray data of all compounds were collected at room temperature on a STOE IPDS I diffractometer (Stoe and Cie GmbH; Darmstadt) with Mo-K_α radiation (0.71073 Å, graphite monochromator). The structures were solved by direct methods and refined after a numerical or semiempirical absorption correction of the diffraction data.[35,36] The SHELX suite of programs was used for all calculations.[37,38] Details concerning the data collection and refinements are summarized in Table 4. Further details of the crystal-structure investigations may be obtained from the Fachinformationszentrum Karlsruhe, D-6344 Eggenstein-Leopoldshafe, Germany, on quoting the depository numbers CSD-420626 (Ln = La), 420627 (Ln = Ce), and 420628 (Ln = Pr). The atomic coordinates, the equivalent displacement parameters, and the site occupancy factors of the three compounds are listed in Table 5 - 7

X-ray powder diffraction

X-ray powder diffraction data were collected on a STOE STADI P diffractometer with Mo-K_α radiation (0.71073 Å) in Debye-Scherrer geometry. The samples were enclosed in silica tubes (0.2 mm), and sealed under argon atmosphere. For pattern fitting (LeBail algorithm) and Rietveld refinement, the GSAS program package [39] was used. The results of the single-crystal X-ray analyses were used as starting models. The crystallographic data and details of the Rietveld refinements are given in Table 8. The isotropic displacement parameters were constrained to be equal for both the two Ln sites (Ln = La, Ce, Pr) and the N and O positions, respectively. Furthermore, the (N,O) site occupancies were fixed. The analyses of the data unequivocally confirmed the purity of the compounds.

Solid-state NMR

Solid-state NMR measurements have been performed on a Bruker Avance DSX 500 spectrometer with an external magnetic field of 11.75 T for $La_3[SiON_3]O$. The ^{29}Si-1D-MAS spectra were recorded with direct excitation using a commercial triple resonance MAS probe, which was equipped with a rotor made of ZrO_2 (diameter: 4 mm). A repetition delay of 4096 s (> $3T_1$) and a rotation frequency of 9 kHZ were chosen. The 90° impulse length was 2.5 µs. The given chemical shift values refer to TMS as external chemical shift reference.

Magnetic Measurements

Magnetic properties of $Ce_3[SiON_3]O$ were measured utilizing a SQUID magnetometer (MPMS-XL Quantum Design Inc.). The sample was inserted in a capsule as fine ground powder which was fitted onto a straw of known diamagnetism. The magnetic susceptibility of the sample was collected between 2 and 300 K with magnetic flux densities up to 0.9 T. The obtained data were corrected for diamagnetic contributions of the capsule, the straw, and the sample using diamagnetic increments and analyzed with a modified Curie-Weiss law $\chi_m = \chi_0 + C/(T - \theta)$. From the Curie constant C, the effective magnetic moment per formula unit is calculated using the spin-only approximation.

Supporting Information: Anisotropic displacement parameters for the three compounds $Ln_3[SiON_3]O$ with Ln = La, Ce, Pr..

Acknowledgements: The authors thank Dr. Oliver Oeckler and Thomas Miller for the collection of the single-crystal data as well as Christian Minke for performing the EDX measurements. The investigations of the magnetical behavior by Prof. Dr. Dirk Johrendt and Daniel Bichler are gratefully acknowledged. Furthermore the authors thank Dr. Jörn Schmedt auf der Günne and Christian Minke for the solid-state NMR measurement. This work was financially supported by the Fonds der Chemischen Industrie (FCI).

Table 1 Results of the MAPLE calculations [kJ/mol] for $Ln_3[SiON_3]O$ (Ln = La, Ce, Pr) based on the O/N distribution in $Gd_3[SiON_3]O$. Δ = difference.

	Ln^{3+}	Si^{4+}	$(N,O)^{2.75-}$	O^{2-}	Total MAPLE	Δ
La:	3957; 4215	10021	4029	1942	40466	0.9
Ce:	4010; 4275	9924	4058	1943	40656	0.4
Pr:	4022; 4295	10000	4078	1955	40878	0.5

Total MAPLE (3 LaN + SiO_2): 40089 kJ/mol

Total MAPLE (3 CeN + SiO_2): 40499 kJ/mol

Total MAPLE (3 PrN + SiO_2): 40670 kJ/mol

Typical partial MAPLE values [kJ/mol]: La^{3+}: 3500 - 5000; Ce^{3+}: 3800 - 4800; Pr^{3+} : 3800 - 4500; Si^{4+}: 9000 - 10200; O^{2-}: 2000 – 2800 ; $(N,O)^{2.75-}$: 4000 – 5200.[23,24]

Table 2 Selected interatomic distances (Å) and angles (°) for $Ln_3[SiN_3O]O$ (Ln = La, Ce, Pr). Standard deviations are given in parentheses.

		La	Ce	Pr
Ln(1)-O(2)[0]	(2x)	2.7684(5)	2.7671(5)	2.7513(5)
Ln(1)-N/O(1)[1]	(8x)	2.858(4)	2.818(3)	2.8078(19)
Ln(2)-N/O(1)[1]	(2x)	2.450(6)	2.411(5)	2.402(3)
Ln(2)-O(2)[0]	(2x)	2.5157(4)	2.4804(4)	2.4701(3)
Ln(2)-N/O(1)[1]	(4x)	2.734(5)	2.712(4)	2.699(3)
Si(1)-N/O(1)[1]	(4x)	1.728(6)	1.736(5)	1.724(3)
N/O(1)[1]-Si(1)-N/O(1)[1]		101.5(4), 113.6(2)	101.1(3), 113.79(17)	101.1(2), 113.83(13)

Table 3 Comparison of the relevant data of isotypic compounds $Ln_3[SiON_3]O$, $Ba_3[SiO_4]O$, $Cs_3[CoCl_4]Cl$ with perovskite.

compound	*a*/*c* ratio	angle ξ / °	deviation from the average X-M distance
$Gd_3[SiON_3]O$	0.603(1)	16.47(1)	5.3 % (X = O, M = Gd)
$Pr_3[SiON_3]O$	0.609(2)	16.53(1)	4.9 % (X = O, M = Pr)
$Ce_3[SiON_3]O$	0.607(2)	16.60(1)	4.9 % (X = O, M = Ce)
$La_3[SiON_3]O$	0.616(2)	16.50(1)	4.3 % (X = O, M = La)
$Cs_3[CoCl_4]Cl$	0.635	19.34	2.4 % (X = Cl, M = Cs)
$Ba_3[SiO_4]O$	0.651	14.96	2.2 % (X = O, M = Ba)
$Ca[TiO_3]$	$2^{-1/2}$	0	none (X = Ti, M = O)

Table 4 Crystallographic data and details of the refinement procedures for $Ln_3[SiON_3]O$ (Ln = La, Ce, Pr). Standard deviations are given in parentheses.

Formula	$La_3[SiON_3]O$	$Ce_3[SiON_3]O$	$Pr_3[SiON_3]O$
Molar mass / g mol^{-1}	518.85	522.48	524.85
Crystal system		tetragonal	
Space group		*I*4/*mcm* (no. 140)	
Cell parameters / Å	a = 6.8224(10)	a = 6.7233(10)	a = 6.6979(9)
	c = 11.074(2)	c = 11.069(2)	c = 11.005(2)
Cell volume / Å^3	515.43(15)	500.33(14)	493.72(14)
Formula units / cell		Z = 4	
X-ray density / g cm^{-3}	6.686	6.936	7.061
Abs. coefficient / mm^{-1}	24.550	26.969	29.275
F(000)	888	900	912
Crystal size / mm^3	0.07 x 0.06 x 0.04	0.08 x 0.05 x 0.04	0.06 x 0.05 x 0.04
Diffractometer		STOE IPDS	
Radiation, monochromator		Mo-K$_\alpha$ (λ = 0.71073Å), graphite	
Temperature / K	293(2)	293(2)	293(2)
2θ range / °	4.22 ≤ θ ≤ 28.47	3.68 ≤ θ ≤ 29.98	3.70 ≤ θ ≤ 30.22
Total no. of reflections	2016	2409	2435
Independent reflections	195	218	220
Observed reflections	164	200	202
Absorption correction	numerical	semiempirical (from equivalents)	numerical
Refined parameters	18	18	18
GOF	1.050	1.152	1.077
R-values [I>2σ(I)]	R1 = 0.0182	R1 = 0.0208	R1 = 0.0131
	wR2 = 0.0363	wR2 = 0.0430	wR2 = 0.0276
all data	R1 = 0.0240	R1 = 0.0234	R1 = 0.0156
	wR2 = 0.0370	wR2 = 0.0435	wR2 = 0.0281
Max. / min. residual electron density / e Å^{-3}	-0.892; 0.962	-1.311; 1.920	-0.763; 0.771

Table 5 Atomic coordinates, equivalent displacement parameters, and site occupancy factors for $La_3[SiN_3O]O$. (T = 293 K). Standard deviations are given in parentheses.

Atom	Wykoff symbol	s.o.f.	*x*	*y*	*z*	U_{eq}
La(1)	4*a*	1	0	0	¼	0.0215(3)
La(2)	8*h*	1	0.67593(5)	0.17593(5)	0	0.0119(2)
Si(1)	4*b*	1	0	1/2	¼	0.0092(7)
N/O(1)	16*l*	0.75; 0.25	0.1387(6)	0.6387(6)	0.1512(6)	0.0179(11)
O(2)	4*c*	1	0	0	0	0.024(3)

Table 6 Atomic coordinates, equivalent displacement parameters, and site occupancy factors for $Ce_3[SiN_3O]O$. (T = 293 K). Standard deviations are given in parentheses.

Atom	Wykoff symbol	s.o.f.	*x*	*y*	*z*	U_{eq}
Ce(1)	4*a*	1	0	0	¼	0.0143(3)
Ce(2)	8*h*	1	0.67548(4)	0.17548(4)	0	0.0059(3)
Si(1)	4*b*	1	0	1/2	¼	0.0057(8)
N/O(1)	16*l*	0.75; 0.25	0.1410(6)	0.6410(6)	0.1504(4)	0.0105(11)
O(2)	4*c*	1	0	0	0	0.021(3)

Table 7 Atomic coordinates, equivalent displacement parameters, and site occupancy factors for $Pr_3[SiN_3O]O$. (T = 293 K). Standard deviations are given in parentheses.

Atom	Wykoff symbol	s.o.f.	*x*	*y*	*z*	U_{eq}
Pr(1)	4*a*	1	0	0	¼	0.01389(15)
Pr(2)	8*h*	1	0.67581(3)	0.17581(3)	0	0.00488(13)
Si(1)	4*b*	1	0	1/2	¼	0.0039(4)
N/O(1)	16*l*	0.75; 0.25	0.1405(4)	0.6405(4)	0.1504(3)	0.0125(6)
O(2)	4*c*	1	0	0	0	0.0233(16)

Table 8 Crystallographic data of $Ln_3[SiN_3O]O$ derived from Rietveld refinement of X-ray data. Standard deviations are given in parentheses.

Formula	$La_3[SiN_3O]O$	$Ce_3[SiN_3O]O$	$Pr_3[SiN_3O]O$
Crystal system		tetragonal	
Space group		*I*4/*mcm* (no. 140)	
Lattice parameters / Å	a = 6.82172(17)	a = 6.72040(10)	a = 6.68498(8)
	c = 11.0981(3)	c = 11.0544(2)	c = 10.99356(17)
Cell volume / $Å^3$	516.46(4)	499.26(2)	491.291(17)
Formula units / cell		$Z = 4$	
Radiation		Mo-K_α (λ = 0.70933Å)	
Profile range / °	$2 \leq 2\theta \leq 50$	$2 \leq 2\theta \leq 60$	$2 \leq 2\theta \leq 60$
No. of data points	4800	5790	5500
Observed reflections	142	218	215
No. of refined parameters	61	60	61
R_p / wR_p	0.0990 / 0.1325	0.0538 / 0.0716	0.0466 / 0.0617
$R_{\|F\|}2$	0.0753	0.0406	0.0458
GOF	0.97	1.36	1.16
Reduced χ^2	0.936	1.842	1.348

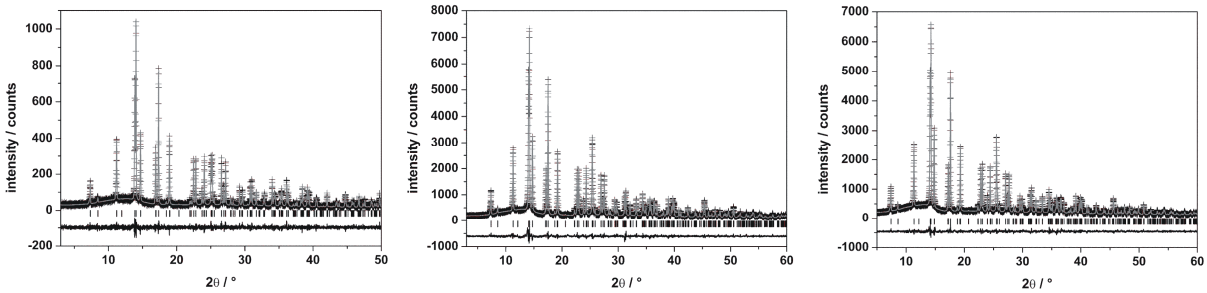

Fig. 1 Observed (crosses) and calculated (line) X-ray powder diffraction patterns as well as difference profile for the Rietveld refinement of $Ln_3[SiON_3]O$ (left: $La_3[SiON_3]O$; middle: $Ce_3[SiON_3]O$; right: $Pr_3SiON_3]O$).

$Pm\bar{3}m$

Si: 1*b* $m\bar{3}m$	O: 1*a* $m\bar{3}m$	Pr: 3*a* $4/mm.m$
½ ½ ½	0 0 0	½ 0 0

↓ *t*3

$P4/mmm$

Si: 1*d* $4/mmm$	O: 1*a* $4/mmm$	Pr: 1*b* $4/mmm$	Pr: 2*f* $mmm.$
½ ½ ½	0 0 0	0 0 ½	0 ½ 0

↓ *k*2 **a-b, a+b, 2c**

$I4/mcm$

Si: 4*b* $\bar{4}2m$	O: 4*c* $4/m$	Pr: 4*d* $m.mm$	Pr: 8*h* $m.2m.$
0 ½ ¼	0 0 0	0 0 ¼	0.67581 0.17581 0

Fig. 2 Crystallographic group-subgroup relation (*Bärnighausen* tree)[40] between $Pr_3[SiON_3]O$ and the perovskite structure type.

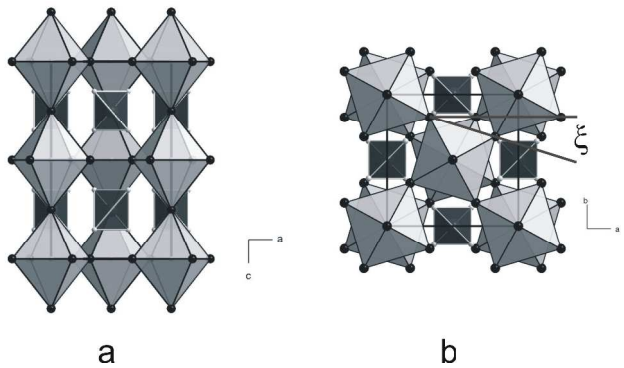

Fig. 3a: Structure of $Ln_3[SiON_3]O$ (Ln = La, Ce, Pr) viewed along [010]. **b:** Structure viewed along [001]; the twisting angle ξ is indicated. The OLn_6 octahedra are depicted light gray, the $SiON_3$ tetrahedra dark gray. The black spheres symbolize Ln^{3+} atoms.

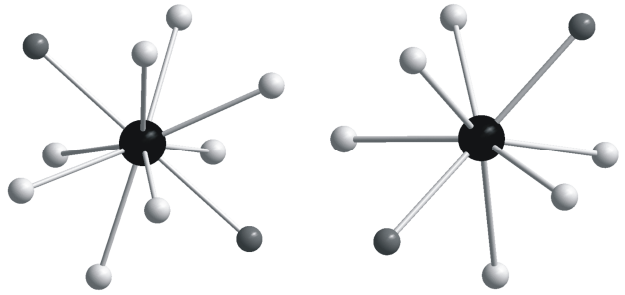

Fig. 4 Coordination spheres of the Ln^{3+} ions (left: Ln(1); right: Ln(2)) (Ln = La, Ce, Pr). (Ln: black; O: light gray; (N,O): dark gray).

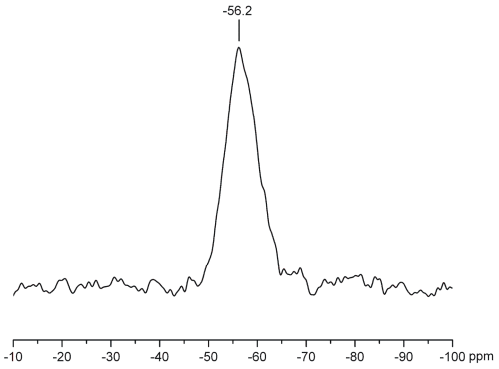

Fig. 5: ^{29}Si solid-state MAS NMR of $La_3[SiON_3]O$.

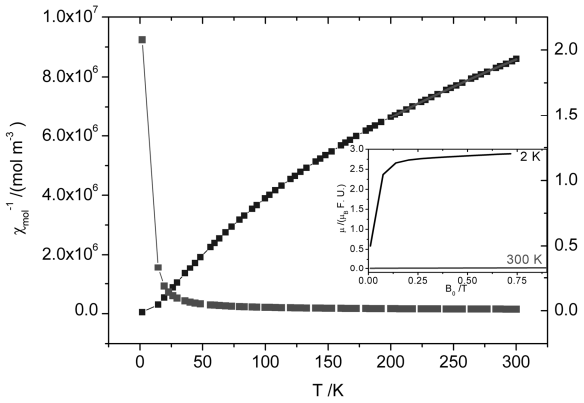

Fig. 6: Temperature dependence of the reciprocal susceptibility (black squares) and the susceptibility (gray squares) of $Ce_3[SiON_3]O$. Insert: Magnetization of $Ce_3[SiON_3]O$ as a function of varying field at different temperatures.

References

[1] O. Bock, U. Müller, *Acta Crystallogr. B* **2002**, *58*, 594.

[2] H. A. Höppe, G. Kotzyba, R. Pöttgen, W. Schnick, *J. Solid State Chem.* **2002**, *167*, 393.

[3] E. Tillmanns, H.-P. Grosse, *Acta Crystallogr. B.* **1978**, *34*, 649.

[4] M. Mansmann, *Z. Anorg. Allg. Chem.* **1965**, *339*, 52.

[5] H. M. Powell, A. F. Wells, *J. Chem. Soc.* **1935**, 359.

[6] H. Huppertz, W. Schnick, *Angew. Chem.* **1996**, *108*, 2115; *Angew. Chem. Int. Ed. Engl.* **1996**, *35*, 1983.

[7] A *dreier* ring can be described as a six-membered ring with *three* tetrahedral centers (e.g. Si) and *three* electronegative atoms (e.g. N), for example. (F. Liebau, *Structural Chemistry of Silicates*, Springer, Berlin, **1985**).

[8] H. A. Höppe, F. Stadler, O. Oeckler, W. Schnick, *Angew. Chem.* **2004**, *116*, 5656; *Angew. Chem. Int. Ed.* **2004**, *43*, 5540.

[9] O. Oeckler, F. Stadler, T. Rosenthal, W. Schnick, *Solid State Sci.* **2007**, *9*, 205.

[10] J. A. Kechele, O. Oeckler, F. Stadler, W. Schnick, *Solid State Sci.* **2009**, *11*, 537.

[11] F. Stadler, O. Oeckler, H. A. Höppe, M. H. Möller, R. Pöttgen, B. D. Mosel, P. Schmidt, V. Duppel, A. Simon, W. Schnick, *Chem. Eur. J.* **2006**, *12*, 6984.

[12] T. Schlieper, W. Schnick, *Z. Anorg. Allg. Chem.* **1995**, *621*, 1037.

[13] T. Schlieper, W. Milius, W. Schnick, *Z. Anorg. Allg. Chem.* **1995**, *621*, 1380.

[14] G. Pilet, H. A. Höppe, W. Schnick, S. Esmaeilzadeh, *Solid State Sci.* **2005**, *7*, 391.

[15] H. Huppertz, W. Schnick, *Chem. Eur. J.* **1997**, *3*, 249.

[16] W. Schnick, H. Huppertz, *Chem. Eur. J.* **1997**, *3*, 679.

[17] W. Schnick, T. Schlieper, H. Huppertz, K. Köllisch, M. Orth, R. Bettenhausen, B. Schwarze, R. Lauterbach, *Phosphorus Sulfur Silicon Relat. Elem.* **1997**, *124/125*, 163.

[18] S. Podsiadlo, *J. Therm. Anal.* **1987**, *32*, 771.

[19] J. Guyader, F. F. Grekov, R. Marchand, J. Lang, *Rev. Chim. Miner.* **1978**, *15*, 431.

[20] R. Marchand, *C. R. Acad. Sci., Ser. IIc: Chim.* **1976**, *283*, 281.

[21] R. Hoppe, *Angew. Chem.* **1966**, *78*, 52; *Angew. Chem. Int. Ed. Engl*. **1966,** *5*, 95.

[22] R. Hoppe, *Angew. Chem.* **1970**, *82*, 7; *Angew. Chem. Int. Ed. Engl*. **1970**, *9*, 25.

[23] H. A. Höppe, *PhD Thesis*, University of Munich, **2003**.

[24] K. Köllisch, *PhD Thesis*, University of Munich, **2001**.

[25] C. Schmolke, S. Lupart, W. Schnick, *Solid State Sci.* **2009**, *11*, 305.

[26] A. Lieb, W. Schnick, *J. Solid State Chem.* **2005**, *178*, 3323.

[27] A. Lieb, R. Lauterbach, W. Schnick, *Z. Anorg. Allg. Chem.* **2006**, *632*, 313.

[28] R. D. Shannon, *Acta Crystallogr. A* **1976**, *32*, 751.

[29] J. Takahashi, H. Yamane, N. Hirosaki, Y. Yamamoto, T. Suehiro, T. Kamiyama, M. Shimada, *Chem. Mater.* **2003**, *15*, 1099.

[30] E. Leonova, A. S. Hakeem, K. Jansson, B. Stevensson, Z. Shen, J. Grins, S. Esmaeilzadeh, M, Edén, *J. Non-Cryst. Solids* **2008**, *354*, 49.

[31] H. Lueken, *Magnetochemie*, Teubner, Stuttgart, **1999**.

[32] W. Schnick, H. Huppertz, R. Lauterbach, *J. Mater. Chem.* **1999**, *9*, 289.

[33] O. Greis, R. Ziel, B. Breidenstein, A. Haase, T. Petzel, *J. Alloys Compds.* **1994**, *216*, 255.

[34] B. Iandelli, *Accademica Nazionale dei Lincei* **1937**, *25*, 129.

[35] *X-Red 32*, Version 1.31, **2005**, STOE and Cie GmbH, Darmstadt.

[36] *X-SHAPE*, Version 2.07, **2005**, STOE and Cie GmbH, Darmstadt.

[37] G. M. Sheldrick, *Acta Crystallogr. A* **2008**, *64*, 112.

[38] L. J. Farrugia, *J. Appl. Crystallogr.* **1999**, *32*, 837.

[39] A. C. Larson, R. B. von Dreele, *GSAS – General Structure Analysis System*, Los Alamos, USA, **1998**.

[40] U. Müller, *Z. Anorg. Allg. Chem.* **2004**, *630*, 1519.